

University of Nebraska - Lincoln

## DigitalCommons@University of Nebraska - Lincoln

---

Mechanical & Materials Engineering Faculty  
Publications

Mechanical & Materials Engineering,  
Department of

---

2010

### Directional annealing-induced texture in melt-spun (Sm<sub>12</sub>Co<sub>88</sub>)<sub>99</sub>Nb<sub>1</sub> alloy

Tanjore V. Jayaraman  
*University of Nebraska-Lincoln*, [tjayaraman2@unl.edu](mailto:tjayaraman2@unl.edu)

P. Rogge  
*University of Nebraska-Lincoln*

Jeffrey E. Shield  
*University of Nebraska-Lincoln*, [jshield@unl.edu](mailto:jshield@unl.edu)

Follow this and additional works at: <https://digitalcommons.unl.edu/mechengfacpub>

 Part of the [Mechanical Engineering Commons](#)

---

Jayaraman, Tanjore V.; Rogge, P.; and Shield, Jeffrey E., "Directional annealing-induced texture in melt-spun (Sm<sub>12</sub>Co<sub>88</sub>)<sub>99</sub>Nb<sub>1</sub> alloy" (2010). *Mechanical & Materials Engineering Faculty Publications*. 43.  
<https://digitalcommons.unl.edu/mechengfacpub/43>

This Article is brought to you for free and open access by the Mechanical & Materials Engineering, Department of at DigitalCommons@University of Nebraska - Lincoln. It has been accepted for inclusion in Mechanical & Materials Engineering Faculty Publications by an authorized administrator of DigitalCommons@University of Nebraska - Lincoln.

## FAST TRACK COMMUNICATION

# Directional annealing-induced texture in melt-spun $(\text{Sm}_{12}\text{Co}_{88})_{99}\text{Nb}_1$ alloy

T V Jayaraman<sup>1,2</sup>, P Rogge<sup>1</sup> and J E Shield<sup>1,2</sup><sup>1</sup> Department of Mechanical Engineering, University of Nebraska, Lincoln, NE 68588, USA<sup>2</sup> Nebraska Center for Materials and Nanoscience, University of Nebraska, Lincoln, NE 68588, USAE-mail: [tjayaraman2@unl.edu](mailto:tjayaraman2@unl.edu)

Received 30 April 2010, in final form 4 May 2010

Published 23 June 2010

Online at [stacks.iop.org/JPhysD/43/272004](http://stacks.iop.org/JPhysD/43/272004)**Abstract**

Developing texture in nanocrystalline permanent magnet alloys is of significant importance. Directional annealing is shown to produce texture in the permanent magnet alloy  $(\text{Sm}_{12}\text{Co}_{88})_{99}\text{Nb}_1$ . Melt spinning produced isotropic grain structures of the hard magnetic metastable  $\text{SmCo}_7$  phase, with grain sizes of  $\sim 300$  nm. Conventional annealing of melt-spun  $(\text{Sm}_{12}\text{Co}_{88})_{99}\text{Nb}_1$  alloy produced  $\text{Sm}_2\text{Co}_{17}$  phase with random crystallographic orientation. Directional annealing of melt-spun  $(\text{Sm}_{12}\text{Co}_{88})_{99}\text{Nb}_1$  alloy, with appropriate combinations of annealing temperature and translational velocity, produced  $\text{Sm}_2\text{Co}_{17}$  phase with (0006) in-plane texture, as determined by x-ray diffraction analysis and magnetic measurements. The magnetization results show out-of-plane remanence higher than the in-plane remanence resulting in the degree of ‘magnetic’ texture in the order of 25–40%. Coercivity values above 2 kOe were maintained. The texture development via directional annealing while minimizing exposure to elevated temperatures provides a new route to anisotropic high-energy permanent magnets.

(Some figures in this article are in colour only in the electronic version)

**1. Introduction**

Sm–Co based magnets have drawn attention since the 1970s for their highly attractive properties, namely high-energy density (15–30 MG Oe), reliable coercive force, best high temperature performance and relatively good corrosion and oxidation resistance. These properties have made these alloys an ideal material in applications such as generators, high speed motors, turbo-machinery, travelling wave tube and applications over a range of temperatures (cryogenic to 180 °C) [1]. Currently nanocomposite Sm–Co based permanent magnets continue to attract interest because of the need for stronger permanent magnets, and the exchange-spring permanent magnets offer the best opportunity to increase the energy products [2]. Rapid solidification of binary Sm–Co alloys results in relatively coarse grain structures [3–5]. However, ternary alloying additions has produced the desired nanoscale two phase structures in rapidly solidified Sm–Co alloys [6–10]. Texture

development while maintaining nanocrystalline grain sizes is challenging with existing processing routes since prolonged exposure to elevated temperatures causes grain growth and subsequent loss of the nanostructure. Texture development using controlled, directional heat transfer has produced texture during both primary crystallization from amorphous precursors and recrystallization of heavily deformed metals and alloys [11–15]. When applied to rapidly solidified permanent magnet alloys, it is expected that the controlled grain growth can produce texture for both bulk and bonded magnet applications.

In the past researchers have reported texture development in nanocrystalline Sm–Co based alloys in a variety of ways including unidirectional solidification, deformation and magnetic field-assisted methods [16, 17]. In this paper we report the observance of (0006) in-plane texture upon directional annealing of rapidly solidified  $(\text{Sm}_{12}\text{Co}_{88})_{99}\text{Nb}_1$  alloy. The effect of directional annealing temperature and

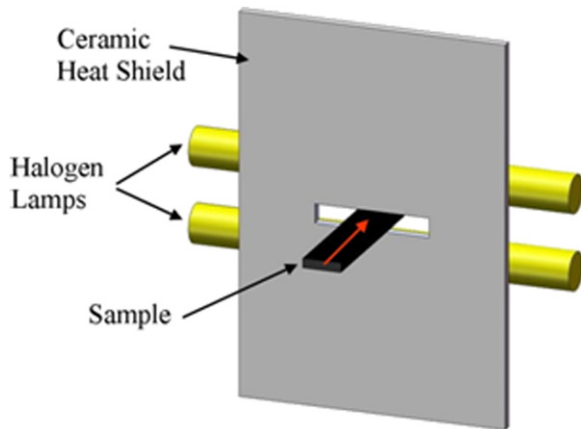


**Figure 1.** Schematic of the experimental set-up for directional annealing. Sample is translated (arrow) past the heat shield and into the furnace.

translational velocity on the development of the texture and its effect on the magnetic properties of this alloy were determined.

## 2. Experimental procedures

### 2.1. Alloy preparation, melt spinning and conventional annealing

Alloy ingots of  $(\text{Sm}_{12}\text{Co}_{88})_{99}\text{Nb}_1$  were prepared from high-purity (>99.95%) elemental constituents (Sm, Co and Nb) by arc-melting in UHP argon atmosphere. An extra 5 wt% Sm was added to account for the vaporization loss of Sm during the melting process. The arc-melted ingots were rapidly solidified by melt spinning at a tangential wheel velocity of  $40 \text{ m s}^{-1}$ . The melt spinning was performed under high-purity argon environment at a chamber pressure of 1 atm. Conventional annealing of melt-spun  $(\text{Sm}_{12}\text{Co}_{88})_{99}\text{Nb}_1$  alloy involved isothermal heat treatment of the ribbon (sealed in a glass tube under UHP Ar) at  $850^\circ\text{C}$  for 10 min.

### 2.2. Directional annealing

The directional annealing was performed on the melt-spun ribbons in a specially designed furnace having a motorized actuator to translate the ribbon (sealed in a glass tube) into the furnace [15]. The dimensions of the melt-spun ribbons were  $7 \text{ mm} \times 2.5 \text{ mm} \times 0.05 \text{ mm}$ . The schematic of the experimental set-up for directional annealing is shown in figure 1. Two halogen lamps (500 W/500 W or a 500 W/1000 W depending on the temperature of the directional annealing process) were enclosed in a furnace made of ceramic bricks. A small opening created in the furnace houses a ceramic plate (MgO). This plate (thickness 1.5 mm) which also acts as a heat shield has a small slit cut to allow the sample to be translated into the furnace. The maximum temperature of the furnace ( $T_{\text{max}}$ ) was controlled by adjusting the voltage of the lamps using a variac.  $T_{\text{max}}$  was measured using a K-type (chromel–alumel) thermocouple located directly between the two halogen lamps. The maximum furnace temperature that could be obtained was  $1200^\circ\text{C}$ . A motorized actuator was used to translate the ribbon (sealed in a glass tube) into the

furnace. The maximum translation distance of the actuator was 12 mm and it was capable of generating a translational velocity ranging from 6 to  $1530 \text{ mm h}^{-1}$ . The temperature gradient in the furnace was dependent on  $T_{\text{max}}$ , when all other parameters of the furnace (namely the heat shield material/thickness and ceramic brick material/thickness) were kept constant. With the heat shield and the ceramic brick materials mentioned above, a temperature gradient of  $82^\circ\text{C mm}^{-1}$  was achieved for a  $T_{\text{max}}$  of  $1000^\circ\text{C}$ . The as-solidified melt-spun ribbons were directionally annealed at various annealing temperatures ( $600\text{--}1100^\circ\text{C}$ ) and translation velocities ( $5\text{--}35 \text{ mm h}^{-1}$ ) combination.

### 2.3. X-ray and magnetic characterization

The melt-spun, conventionally annealed and directionally annealed melt-spun ribbons were analysed by a Rigaku MultiFlex x-ray diffractometer with  $\theta\text{--}\theta$  geometry using  $\text{Cu K}\alpha$  radiation. The magnetic property measurements were performed using Quantum Design Magnetic Property Measurement System (MPMS-XL) magnetometer. The magnetization curves were obtained at room temperature (300 K) with a maximum field of 7 T. They were performed on the ribbon samples both in-plane (parallel and perpendicular to the long axis of the ribbon) and out-of-plane (perpendicular to the plane of the ribbon). The magnetization curves were corrected for self-demagnetizing fields that arise due to the shape of the ribbon and the direction of the applied field.

## 3. Results and discussions

### 3.1. X-ray and magnetization results for melt-spun and conventionally annealed ribbons

The x-ray diffraction pattern, magnetization curves and microstructure for the melt-spun  $(\text{Sm}_{12}\text{Co}_{88})_{99}\text{Nb}_1$  have been previously reported [10, 18].  $\text{Sm}_{12}\text{Co}_{88}$  modified with 1 at% Nb obtained by rapid solidification using melt spinning resulted in an isotropic structure with a grain size of approximately 300 nm having remanence  $\sim 6 \text{ kG}$  and coercivity  $\sim 8 \text{ kOe}$  [10]. While the melt-spun  $(\text{Sm}_{12}\text{Co}_{88})_{99}\text{Nb}_1$  alloy formed the metastable  $\text{TbCu}_7$ -type  $\text{SmCo}_7$  structure [18], conventional annealing of melt-spun  $(\text{Sm}_{12}\text{Co}_{88})_{99}\text{Nb}_1$  alloy ribbon resulted in the formation of the rhombohedral  $\text{Th}_2\text{Zn}_{17}$ -type  $\text{Sm}_2\text{Co}_{17}$  structure [19]. Figure 2 shows the x-ray diffraction spectra and the magnetization curves for conventionally annealed ribbon. While the crystal structure of  $\text{Sm}_2\text{Co}_{17}$  is rhombohedral, the hexagonal indexing scheme [20] has been used here since it more readily identifies the  $c$ -axis texture. The x-ray diffraction peak intensities indicate an isotropic structure. Similarly, the magnetization curves, figure 2(b), show the presence of an isotropic structure in the conventionally annealed ribbon having remanence  $\sim 5 \text{ kG}$  and coercivity  $\sim 4.5 \text{ kOe}$ .

### 3.2. X-ray diffraction results for directionally annealed ribbon

Directional annealing was performed on melt-spun  $(\text{Sm}_{12}\text{Co}_{88})_{99}\text{Nb}_1$  alloy ribbons at various annealing temperatures ( $600\text{--}1200^\circ\text{C}$ ) and translational velocities ( $5\text{--}35 \text{ mm h}^{-1}$ )

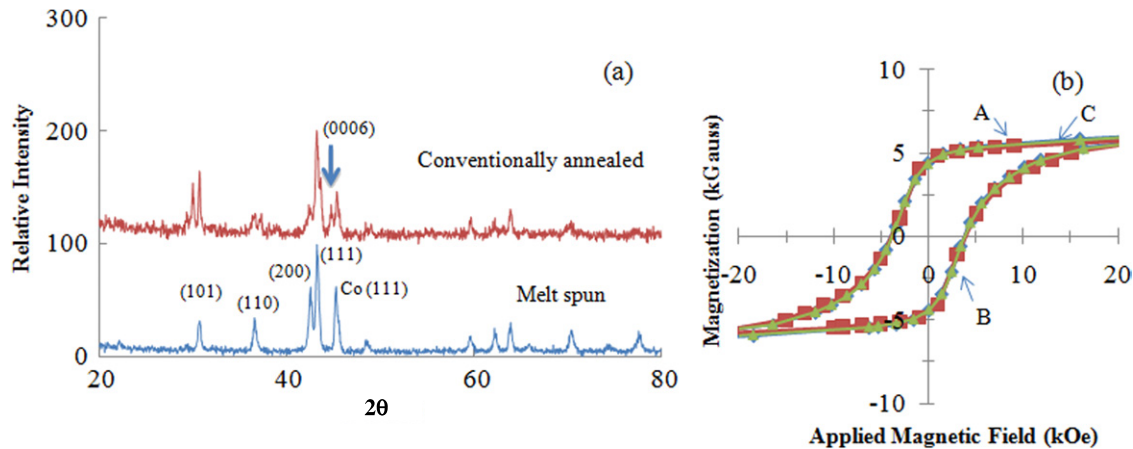


**Figure 2.** (a) X-ray diffraction spectra of melt-spun and conventionally annealed melt-spun ( $\text{Sm}_{12}\text{Co}_{88}$ ) $_{99}\text{Nb}_1$  ribbons. (b) Magnetization curves for conventionally annealed melt-spun ( $\text{Sm}_{12}\text{Co}_{88}$ ) $_{99}\text{Nb}_1$  alloy ribbon: out-of-plane perpendicular to the ribbon [A], in-plane parallel and perpendicular to the long axis of the ribbon, [B] and [C], respectively.

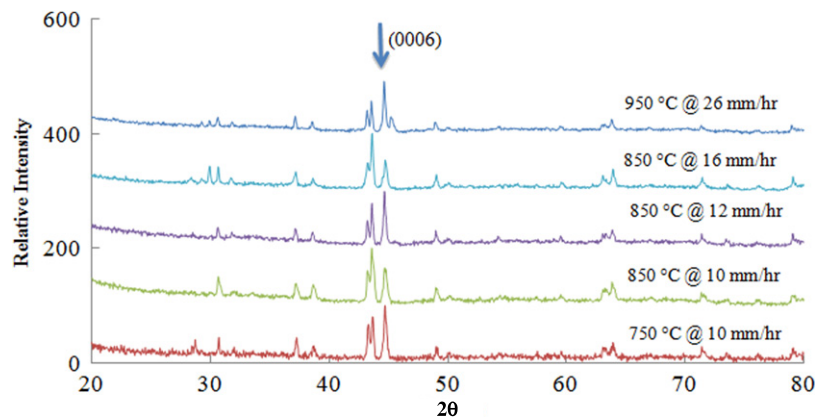


**Figure 3.** X-ray diffraction spectra of directionally annealed melt-spun ( $\text{Sm}_{12}\text{Co}_{88}$ ) $_{99}\text{Nb}_1$  alloy ribbons.

combinations. Figure 3 shows the x-ray diffraction spectra of the directionally annealed ( $\text{Sm}_{12}\text{Co}_{88}$ ) $_{99}\text{Nb}_1$  alloy at annealing temperatures 750, 850 and 950 °C. Similar to conventionally annealed ribbon, the original TbCu<sub>7</sub>-type structure in as-solidified melt-spun ribbons has transformed to  $\text{Sm}_2\text{Co}_{17}$  for directionally annealed ribbons. The development of (0006) in-plane texture was observed at translational velocities 10 mm h<sup>-1</sup>, 12 mm h<sup>-1</sup> and 26 mm h<sup>-1</sup>, for temperatures 750 °C, 850 °C and 950 °C, respectively. It can be observed that with an increase in directional annealing temperature, texture development occurred at higher translational velocity. The enhanced (0006) diffraction peak is observed in directionally annealed ribbons and not in melt-spun and conventionally annealed melt-spun ribbons. The basal planes lie preferentially in the ribbon plane so that the [0001] easy magnetization direction points out-of-plane. It may be noted that the directional annealing was performed at each temperature over a range of translational velocities; however, the texture was observed at only certain combinations of annealing temperature and translation velocity, indicating distinct processing windows in which texture development occurs. For a directional annealing temperature 850 °C a translational velocity of 12 mm h<sup>-1</sup> leads to development of (0006) in-plane texture. However, at lower and higher translational velocities, 10 mm h<sup>-1</sup> and

16 mm h<sup>-1</sup>, respectively, one can observe the tendency for the (0006) in-plane texture formation. At lower translational velocity (10 mm h<sup>-1</sup>) the exposure time at the directional annealing temperature (850 °C) is higher than that for a translational velocity 12 mm h<sup>-1</sup>, leading to isotropic grain growth after initial texture development and subsequent loss of the texture. At higher translational velocity (16 mm h<sup>-1</sup>) the exposure time at the directional annealing temperature (850 °C) is less, leading to incomplete texture formation.

The development of texture indicates that there is mobility advantage of the energetically favoured boundaries as compared to the normal grain growth in the processing window where texture is observed [21]. Mobility advantage depends on the hot zone velocity, temperature gradient and activation energy [22, 23]. In this study the temperature gradient along the ribbon and the translational velocity of the ribbon dictate the mobility advantage for the texture and the temperature gradient along the sample during directional annealing is solely dependent on the directional annealing temperature. The temperature gradients observed were 64 °C mm<sup>-1</sup>, 73 °C mm<sup>-1</sup> and 81 °C, for a  $T_{\text{max}}$  of 750 °C, 850 °C and 950 °C, respectively. The ability to vary thermal gradient for a particular temperature can increase the



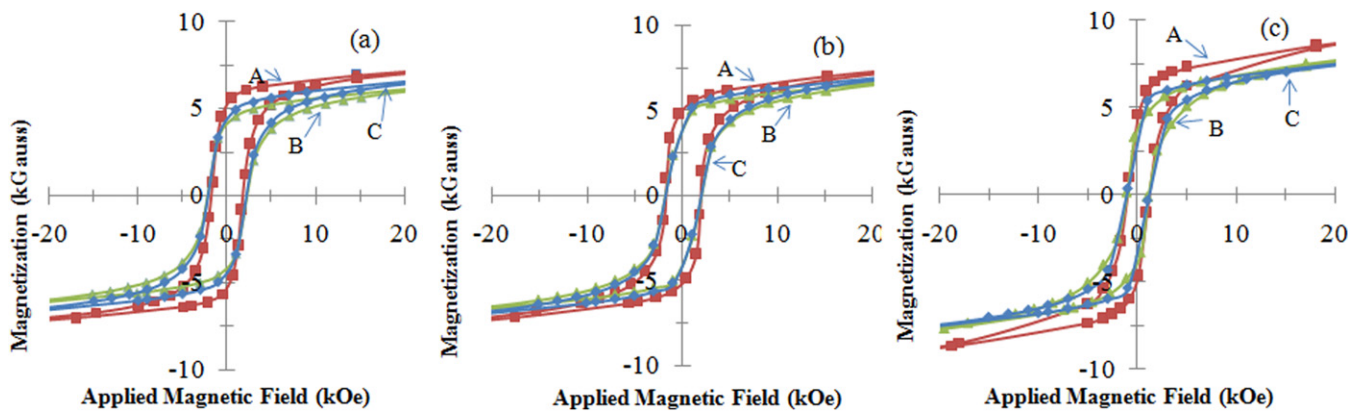


**Figure 4.** Magnetization curves for directionally annealed melt-spun  $(\text{Sm}_{12}\text{Co}_{88})_{99}\text{Nb}_1$  alloy ribbons: (a)  $750^\circ\text{C}$  at  $10\text{ mm h}^{-1}$ , (b)  $850^\circ\text{C}$  at  $12\text{ mm h}^{-1}$  and (c)  $950^\circ\text{C}$  at  $26\text{ mm h}^{-1}$ . [A] out-of-plane perpendicular to the ribbon, [B] in-plane parallel to the long axis of the ribbon and [C] in-plane perpendicular to the long axis.

processing window and have better control over the texture development.

### 3.3. Magnetization results for the directionally annealed ribbon

Figure 4 shows the magnetization curves for directionally annealed melt-spun  $(\text{Sm}_{12}\text{Co}_{88})_{99}\text{Nb}_1$  ribbons. The magnetic measurements were performed on the same ribbons on which the x-ray diffraction spectra were obtained. It can be observed that the magnetization curves for the directionally annealed ribbons that showed texture in x-ray diffraction spectra show out-of-plane remanence higher than the in-plane remanence: 5.5 kG and 4.0 kG ( $750^\circ\text{C}/10\text{ mm h}^{-1}$ ), 5.0 kG and 4.0 kG ( $850^\circ\text{C}/12\text{ mm h}^{-1}$ ) and 4.5 kG and 3.5 kG ( $950^\circ\text{C}/26\text{ mm h}^{-1}$ ), respectively. The degree of ‘magnetic’ texture can be approximated by the ratio of difference between out-of-plane and in-plane remanence to the in-plane remanence [16], which in this case are in the order of 25–40% for the directionally annealed ribbons. However, there is appreciable decrease in coercivity of directionally annealed ribbons ( $\sim 2\text{--}3\text{ kOe}$ ) as compared with conventionally annealed ribbon (4 kOe). This may be due to grain growth in the directionally annealed samples which results in a lower coercivity. The fact that directional annealing at higher temperatures results in the lowest coercivities supports this hypothesis. Further optimization of the experimental set-up to limit the grain growth is underway.

## 4. Conclusions

Directional annealing of rapidly solidified  $(\text{Sm}_{12}\text{Co}_{88})_{99}\text{Nb}_1$  alloy ribbons resulted in the development of the (0006) in-plane texture, as shown by both x-ray diffraction and magnetometry. The development of texture was sensitive to annealing temperature and translational velocity, including  $10\text{ mm h}^{-1}$ ,  $12\text{ mm h}^{-1}$  and  $26\text{ mm h}^{-1}$ , for temperatures  $750^\circ\text{C}$ ,  $850^\circ\text{C}$  and  $950^\circ\text{C}$ , respectively. The magnetization results show out-of-plane remanence higher than the in-plane remanence. The degree of ‘magnetic’ texture ranged between 25–40% for the directionally annealed ribbons, depending

on processing conditions. No texture was observed in melt-spun and conventionally annealed (isothermal heat treatment at  $850^\circ\text{C}$  for 10 min) ribbons. This study shows a feasible process for developing texture in nanocrystalline permanent magnet alloys by directional annealing.

## Acknowledgments

The authors gratefully acknowledge the research support from the Department of Defense Office of Naval Research under grant no N00014-09-1-0620.

## References

- [1] Cullity B D and Graham C D 2009 *Introduction to Magnetic Materials* (Hoboken, NJ: Wiley/IEEE Press)
- [2] Skomski R and Coey J M D 1993 *Phys. Rev. B* **48** 15812
- [3] Chen C H, Kodat S, Walmer M H, Cheng S F, Willard M A and Harris V G 2003 *J. Appl. Phys.* **93** 7966
- [4] Chen S K, Chu M S and Tsai J L 1996 *IEEE Trans. Magn.* **32** 4419
- [5] Ravindran V K and Shield J E 2007 *Met. Trans. A* **38** 732
- [6] Manrakkhan W, Withanawasam L, Meng-Burany X, Gong W and Hadjipanayis G C 1997 *IEEE Trans. Magn.* **33** 3898
- [7] Makridis S S, Litsardakis G, Panagiotopoulos I, Niarchos D, Zhang Y and Hadjipanayis G C 2002 *IEEE Trans. Magn.* **38** 2922
- [8] Gopalan R, Ping D H and Hono K 2004 *J. Magn. Magn. Mater.* **284** 321
- [9] Makridis S S, Panagiotopoulos I, Tsiaoussis I, Frangis N, Pavlidou E, Chrisafis K, Papathanasiou G F, Efthimiadis K, Hadjipanayis G C and Niarchos D 2008 *J. Magn. Magn. Mater.* **320** 2322
- [10] Aich S and Shield J E 2006 *J. Alloys Compounds* **425** 416
- [11] Kim S J, Birnie III D P, Zelinski B J J and Uhlmann D R 1995 *J. Non-Cryst. Solids* **181** 291
- [12] Baker I and Li J 2002 *Acta Mater.* **50** 805
- [13] Li J, Johns S L, Illiescu B M, Frost H J and Baker I 2002 *Acta Mater.* **50** 4491
- [14] Zhang Z W, Chen G L and Chen G 2006 *Mater. Sci. Eng. A* **422** 241
- [15] Rogge P 2008 *BS (Honours) Thesis* Department of Mechanical Engineering, University of Nebraska, Lincoln
- [16] Gabay A M, Marinescu M, Lui J F and Hadjipanayis G C 2009 *J. Magn. Magn. Mater.* **321** 3318

- [17] Pligaru N, Rubin J and Bartolome J 2007 *J. Alloys Compounds* **433** 129
- [18] Buschow K H J and van der Goot A S 1971 *Acta Crystallogr. Sect. B: Struct. Crystallogr. Cryst. Chem.* **27** 1085
- [19] Beller Kostogorova Y Y, Shield J E and Kramer M J 2007 *J. Appl. Phys.* **101** 09K521
- [20] Cullity B D and Stock S R 2001 *Elements of X-Ray Diffraction* (Englewood Cliffs, NJ: Prentice-Hall)
- [21] Godfrey A W and Martin J W 1995 *Phil. Mag. A* **72** 737
- [22] Holm E A, Zacharopoulos N and Srolovitz D J 1998 *Acta Mater.* **46** 953
- [23] Badmos A Y, Frost H J and Baker I 2002 *Acta Mater.* **50** 3347